Research Article

Akira Yabe*

Desensitization of axially asymmetric optical systems

Abstract: Axially asymmetric optical systems treated in this paper contain both freeform surfaces and spheres. In these systems, freeform surfaces need to be allocated at the most effective position. The problem can be elegantly solved with the method of traveling freeform surfaces. The purpose of this paper is to show that the sensitivity control can be included in this design process.

Keywords: decenter; freeform surface; optimization; surface irregularity; tolerance sensitivity.

OCIS codes: 220.2740; 220.3620; 220.1250.

***Corresponding author: Akira Yabe**, Habichtstr. 58, 86899 Landsberg, Germany, e-mail: akira.yabe@t-online.de

1 Introduction

For the practical use of axially asymmetric optical systems, the sensitivity to manufacture errors is a critical factor. The alignment of axially asymmetric elements is a challenging as is the manufacturing of freeform surfaces. To realize performance in the products, the sensitivity to misalignment and surface error need to be reduced as much as possible during the design phase. Some might discuss that the appropriate selection of compensators would be more important to realize the good as-built performance than the reduction of the sensitivity. But the compensation is not perfect, and the residual defect is smaller if the sensitivity is smaller, in general. The reduction of the sensitivity is important in this context, too.

The methods to get the insensitive optical systems could be classified as follows. In the first class, the influence of the manufacturing errors is investigated analytically for individual optical systems [1]. In the second class, the nominal system and the perturbed systems are simultaneously optimized [2]. In the third class, the most insensitive design is picked up from many solutions of the global optimization [3]. In the fourth class, a sensitivity control function is constructed for the optimization [4]. In the first method, the special consideration is required for each case. The obtained result is not always general. In the second method, a lot of calculation time is required for the evaluation of the perturbed systems. The number of the perturbed systems is limited practically. In the third method, an occasionally insensitive design is picked up from among many solutions, which were obtained without sensitivity control. The author proposed a general method of sensitivity control for manufacturing errors in 2010 [5]. In this method, the target function to exactly express the effect of manufacturing errors is introduced. This method is general and can be applied to axially asymmetric systems.

The author also proposed a method of sensitivity control to surface irregularity in 2006 [6]. This method can be applied to the shape error of freeform surfaces. In this method, orthogonal base functions are defined to express the surface irregularity. In 2007, Forbes proposed two types of orthogonal functions to express the asphere shape, which he named Qcon and Qbfs [7]. Qcon is just what the author introduced for sensitivity control to surface irregularity in his paper. Youngworth investigated the effectiveness of orthogonal functions for tolerancing of surface irregularity [8]. Forbes established the measure of the manufacturability of aspheres [9]. The better manufacturability means the smaller manufacturing error under the given cost. The reduction of the sensitivity means a smaller loss of performance under the given manufacturing error. Both considerations are necessary to achieve the good as-built performance.

The author proposed a representation of freeform surfaces suitable for optimization in 2012 [10]. This representation consists of the rotationally asymmetric quadric and orthogonal polynomials with terms of more than the second order of the coordinate variables. The orthogonal polynomials are the modification of the Zernike polynomials. The first-order terms are not included because they are treated as the tilt of the surface. The second-order terms are not included because they are included in the rotationally asymmetric quadric. These features are favorable for the optimization because the tilt, the paraxial properties,

and the higher-order terms are clearly separated. These polynomials are the extension of the orthogonal functions introduced by the author for sensitivity control to surface irregularity. This representation is also suitable for sensitivity control to surface irregularity.

The author proposed a method to allocate freeform surfaces in axially asymmetric optical systems in 2011 [11]. The manufacturing cost of freeform surfaces is much higher than that of spheres. The number of freeform surfaces should be as small as possible. The freeform surfaces should be used at the most effective position in the optical system. The traveling freeform surface has a real-number surface number, which can be used as an independent variable of the optimization. The optimal position of freeform surfaces can be found through ordinary optimization, just as the surface curvatures or surface separations are determined. The purpose of this paper is to describe the method of sensitivity control in optical systems with traveling freeform surfaces. This is described in section 2.

The design example is a rear projection lens with a mirror. The sensitivity to decenter and surface irregularity are controlled. The designs with and without the sensitivity control are compared, and the effect of the sensitivity control is demonstrated. This is described in section 3.

2 Method

First, the concept of the traveling freeform surface is explained [11]. The purpose of the traveling freeform surface is to include the freeform surface number in the independent variables of the optimization. For the ordinary optimization methods, such as the damped least square method and the global optimization with escape function [12], the independent variables need to be real numbers. The freeform surface number is the integer, but it needs to be extended to the real number. The optical system with the real-number freeform surface number needs to be defined and evaluated.

Figure 1A shows a singlet with a freeform surface at the front surface. Figure 1B shows a singlet with a freeform surface at the rear surface. The freeform surface number is 1 for Figure 1A and 2 for Figure 1B. The role of the overlapped dummy surfaces will be explained later. Figure 1C shows a singlet with a freeform surface number of 1.5. Table 1A, 1B, and 1C show the lens data of Figure 1A, 1B, and 1C, respectively. C1 and C2 are the curvatures of surfaces 1 and 2. D1 and D2 are the surface separations after surfaces 1 and 2. N1 is the refractive index after surface 1. T is the tilt angle. These lens data have the same structure. The surfaces 1 and 2 are spheres without the tilt. The surfaces ‘a’ and ‘b’ are freeform surfaces with the tilt, which are inserted between surfaces 1 and 2. The position and the shape of surfaces ‘a’ and ‘b’ correspond to the real-number surface number, shape, and tilt of the freeform surface. In Table 1A, surfaces 1 and ‘a’ overlap and do not affect the ray trace. The surface ‘b’ represents the freeform surface. In Table 1B, surfaces ‘b’ and 2 overlap and do not affect the ray trace. The surface ‘a’ represents the freeform surface. The shape and position of surfaces ‘a’ and ‘b’ change continuously from Table 1A to Table 1B through Table 1C. The freeform surface shape is shared in surface ‘a’ and ‘b’ in Table 1C. The freeform surface shape is proportional to each other for ‘a’ and ‘b’ because there is the freedom of shape for only one surface. The factors in the parentheses show this relation. The difference of the factors of ‘b’ and ‘a’ is always 1. Therefore, the factor of ‘a’ in Table 1B is -1. When the lens data is interpreted as a traditional optical system, the freeform surface shape of ‘a’ in Table 1B is the minus of the freeform surface shape of

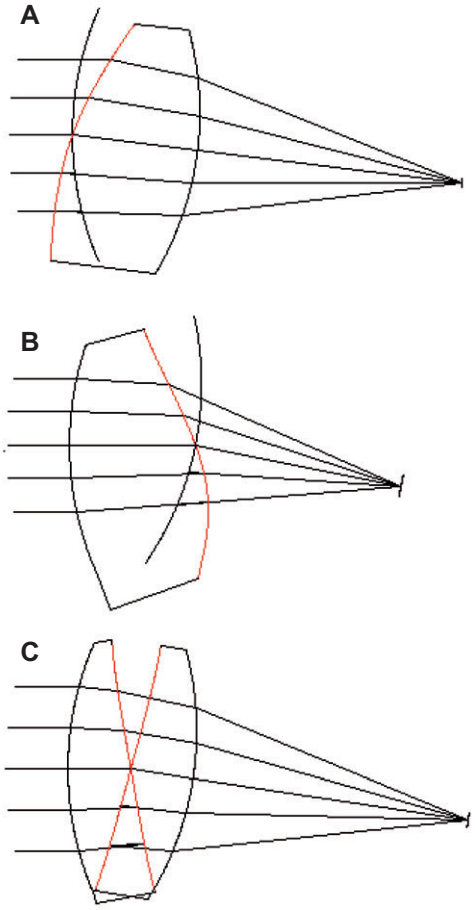

Figure 1 (A) Singlet with the freeform surface number 1. (B) Singlet with the freeform surface number 2. (C) Singlet with the freeform surface number 1.5.

Table 1A Lens data for singlet with freeform surface number 1.

Surf.	Curv.	Dist.	Index	Tilt	
1	C1	0	N1	0	
a	C1	0	1	0	
b	C1	D1	N1	T	Freeform (f)
2	C2	D2	1	0	

Table 1B Lens data for singlet with freeform surface number 2.

Surf.	Curv.	Dist.	Index	Tilt	
1	C1	D1	N1	0	
a	C2	0	1	-T	Freeform (-f)
b	C2	0	N1	0	
2	C2	D2	1	0	

Table 1C Lens data for singlet with freeform surface number 1.5.

Surf.	Curv.	Dist.	Index	Tilt	
1	C1	D1/2	N1	0	
a	(C1+C2)/2	0	1	-T/2	Freeform (-1/2f)
b	(C1+C2)/2	D1/2	N1	T/2	Freeform (1/2f)
2	C2	D2	1	0	

the 'traveling' freeform surface. The real-number freeform surface number in the air space is defined in a similar way. From the definition, the aberration of the optical system with the real-number surface number is continuous to the real-number surface number. The smoothness within the glass space and within the air space is trivial. The smoothness at the boundary of the glass space and the air space can be assured by relating the surface number and the position of inserted surfaces appropriately. More details are given in the original papers [11, 13].

During the optimization, the control of values calculated on a surface might be necessary. Examples are the maximum ray height on the surface or the maximum deviation of the aspherical shape from the best-fit sphere. For the sensitivity control, the γ factor of each sample ray need to be calculated at each surface [5]. The Γ factor is defined as

$$\Gamma = N'\mathbf{l}'\cdot\mathbf{n} - N\mathbf{l}\cdot\mathbf{n} \tag{1}$$

where $\mathbf{n}$ is the unit vector normal to the surface at the point of the refraction, $\mathbf{l}$ is the direction vector of the incident ray, $\mathbf{l}'$ is the direction vector of the refracted ray, and N and N' are the refractive indices before and after the surface. It should be noticed that the total lens number does not change, even if traveling freeform surfaces are included in the optical system. The traveling freeform surface influences the values on the surfaces just before and just after the traveling freeform surface number. This influence need to be continuous to the real-number surface number. The notation of surfaces 1 and '1' is used in a different meaning. Surface 1 is the sphere without the tilt. Surface '1' is the surface affected by the traveling freeform surface with the surface number between 1 and 2. Surface 2 is the sphere without the tilt. Surface '2' is the surface affected by the traveling freeform surface with the surface number between 1 and 2. In Table 1A, surface 'b' represents the freeform surface. As the values of surface '1', the values of surface 'b' should be used.

$$\Gamma_{'1'} = \Gamma_b, \quad \Gamma_{'2'} = \Gamma_2 \tag{2}$$

In Table 1B, surface 'a' represents the freeform surface. As the values of surface '2', the values of surface 'a' should be used.

$$\Gamma_{'1'} = \Gamma_1, \quad \Gamma_{'2'} = \Gamma_a \tag{3}$$

With the consideration of the continuity, the values of surfaces '1' and '2' in Table 1C should be defined as the interpolation of the values of Table 1A and 1B. Therefore, the value of surface '1' is the average of the values of surfaces 1 and 'b,' and the value of surface '2' is the average of the values of surfaces 2 and 'a'.

$$\Gamma_{'1'} = (\Gamma_1 + \Gamma_b)/2, \quad \Gamma_{'2'} = (\Gamma_2 + \Gamma_a)/2 \tag{4}$$

3 Example

The design example is a rear projection lens with a mirror [13]. Figure 2 shows the configuration of the screen,

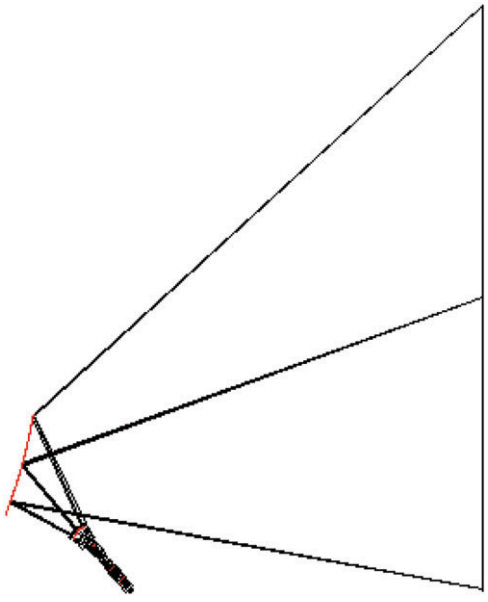

Figure 2 Configuration of screen, mirror, and projection lens.

Table 2 Specification of the example.

Screen size 960 mm×720 mm
Source size 17.6 mm×13.2 mm
Distance between the screen and the projection lens 1500 mm
F-number 2.4
Sample wave lengths 540 nm 450 nm 630 nm
MTF >84% at 36 lp/mm
Distortion <0.3%

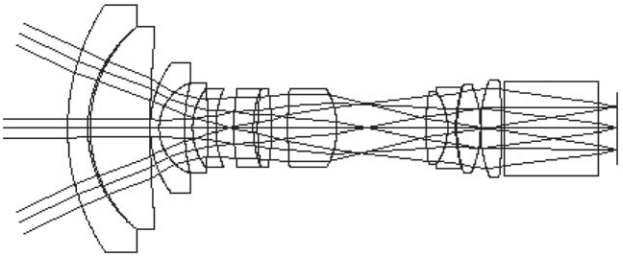

Figure 3 Starting point of the design.

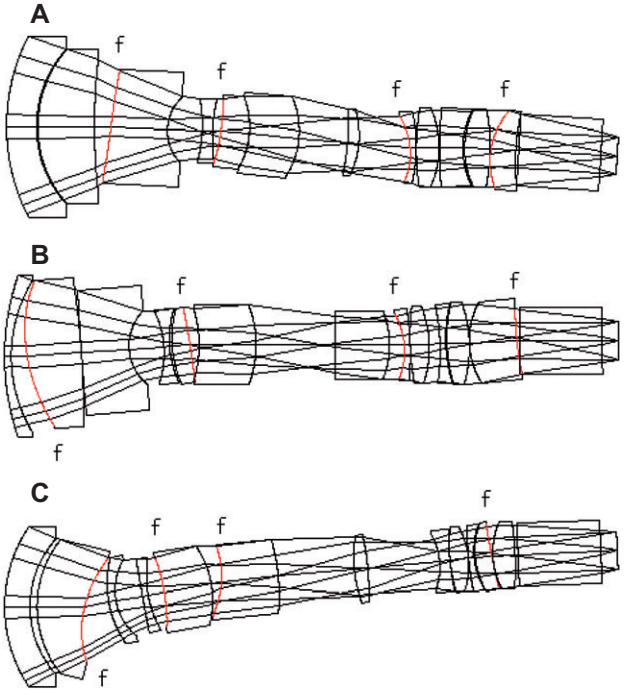

Figure 4 (A) Design without the sensitivity control. (B) Design with the sensitivity control to decenter. (C) Design with the sensitivity control to decenter and surface irregularity.

mirror, and projection lens. The screen is tilted to the optical axis, and the mirror is supposed to be a freeform surface. Table 2 shows the specifications of the example. Figure 3 shows the starting point of the design, which is axially symmetric. The rays are drawn for the off-axis field points, which correspond to the vertical edges (0.6×full

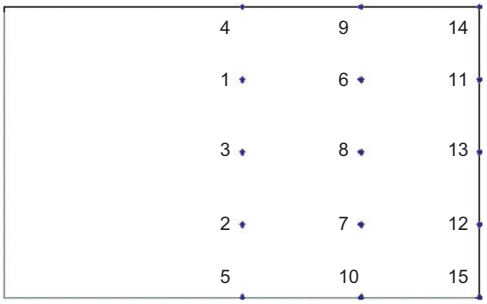

Figure 5 Sample field points.

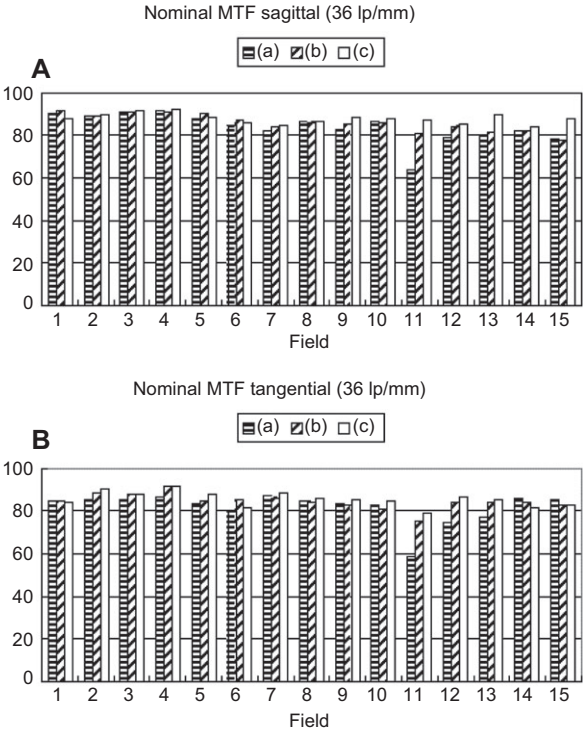

Figure 6 (A) Nominal MTF (sagittal). (B) Nominal MTF (tangential).

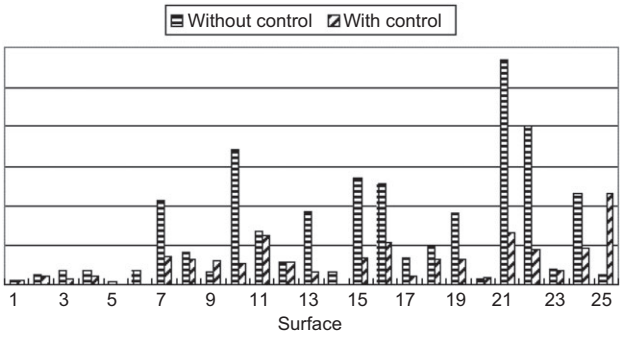

Figure 7 Decenter sensitivity at each surface.

field). The projection lens need to be axially asymmetric to correct the keystone distortion caused by the tilt of the screen. The number of the freeform surfaces is assumed to

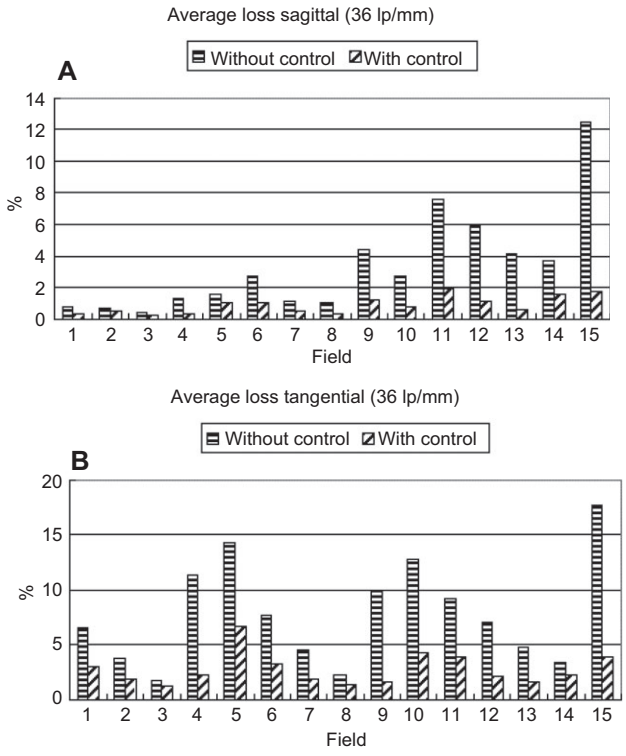

Figure 8 (A) Average MTF loss at each field by decenter (sagittal). (B) Average MTF loss at each field by decenter (tangential).

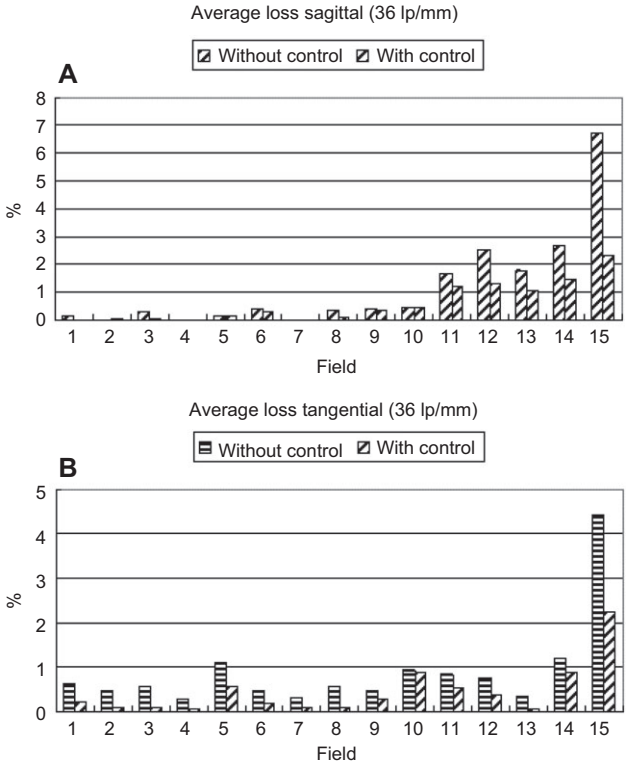

Figure 10 (A) Average MTF loss at each field by surface irregularity (sagittal). (B) Average MTF loss at each field by surface irregularity (tangential).

be 4. The position of the freeform surfaces is determined by the optimization with the traveling freeform surfaces. The freeform surface shape is expressed with orthogonal polynomials up to the eighth order [3].

The target function, which expresses the effect of the manufacturing errors to the root mean square optical path difference (RMS OPD) was controlled during the global optimization and the modulation transfer function (MTF) optimization [5, 12, 14]. Figure 4 shows the designs with the different sensitivity control. Figure 4A is the design without the sensitivity control. Figure 4B is the design with the sensitivity control to decenter. Figure 4C is the design with the sensitivity control to decenter and surface irregularity. The freeform surfaces are labeled with 'f'. The surface apertures were determined with the rays for the vertical edge fields. Figure 5 shows the location of sample field points and their labels. If this is viewed as the position on the source surface, the upper side corresponds to the upper side of Figure 4. The upper side is projected to the lower side of the screen of Figure 2. Figure 6 shows the nominal MTF of three designs. It may look strange that the nominal MTF of the design (a) is lower than designs (b) and (c). This is because the solution number of the global optimization is not enough to get the best design for each case.

Figure 7 shows the comparison of the decenter sensitivity between designs (a) and (b). The decenter sensitivity is defined by the square root of the increase of the expectation value of the variance of OPD under the decenter [5]. The decenter at each surface is supposed to be statistically independent and have the same variance. The value is of the central wavelength. It has the dimension of the length. The value is proportional to the standard deviation of the decenter. The scaling is not important for the purpose of the sensitivity control.

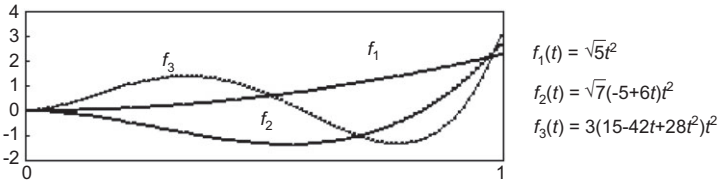

Figure 9 Base functions of surface irregularity.

Table 3A Lens data for the design (a).

	Radius of curvature	Thickness	n (540 nm)	n (450 nm)	n (630 nm)
1	-1199.2907634	227.2323352			
2	69.1119790	10.5868763	1.85996	1.89091	1.84318
3	40.8983468	0.4600309			
4	41.1870810	19.9881973	1.74426	1.75558	1.73748
5	215.8742891	5.8185214			
6	-1129.9691740	19.9269065	1.49167	1.49638	1.48880
7	15.9915201	12.3025787			
8	-47.2239237	3.6129436	1.53897	1.54792	1.53371
9	56.1490505	2.9483845			
10	-87.5014696	10.0474302	1.85656	1.87613	1.84543
11	-29.3862977	0.0620620			
12	-28.9193917	17.5050531	1.49167	1.49637	1.48880
13	-30.1048865	17.2876183			
14	-82.3594157	3.9575926	1.49167	1.49637	1.48880
15	-31.8011769	18.1277646			
16	-24.5286160	2.2181889	1.82543	1.83972	1.81694
17	-55.3686306	-0.0000256			
18	89.5638207	8.0209066	1.50929	1.51434	1.50621
19	-34.1693489	0.1595877			
20	139.6002674	8.2416947	1.75630	1.77485	1.74578
21	29.3280061	0.6059832			
22	31.2764246	9.0993455	1.49453	1.49928	1.49162
23	-64.6690044	0.2567733			
24	25.6550661	8.7655858	1.49167	1.49638	1.48880
25	81.9235238	1.0000000			
26	INFINITY	29.0000000	1.51857	1.52485	1.51472
27	INFINITY	5.8004000			
1	TILT	IN	35.0000000	OUT	-35.0000000
K	1.000000000000E+00				
X0Y3	0.868352664614E-06	X0Y4	-0.127242616771E-07	X0Y5	-0.658577102328E-11
X0Y6	0.107924977387E-11	X0Y7	-0.740062055160E-15	X0Y8	-0.216998512636E-16
X2Y0	-0.227644769839E-04	X4Y0	-0.533966050033E-08	X6Y0	0.191650857549E-12
X8Y0	-0.989923020321E-18				
X2Y1	-0.774238653282E-06	X2Y2	0.940812974001E-08	X2Y3	0.254740656822E-11
X2Y4	-0.453937918109E-13	X2Y5	-0.541436110968E-15	X2Y6	0.464923959753E-17
X4Y1	0.724723173441E-10	X4Y2	-0.237596650561E-12	X4Y3	-0.129098321457E-15
X4Y4	-0.871317340427E-18	X6Y1	-0.200232217976E-14	X6Y2	0.754485359195E-17
6	TILT	IN	-4.9863659	OUT	-7.4496120
K	1.000000000000E+00				
X0Y3	0.675067808416E-04	X0Y4	0.277420373840E-05	X0Y5	-0.438008889930E-07
X0Y6	-0.348170673024E-08	X0Y7	0.404817414838E-10	X0Y8	0.262767498037E-11
X2Y0	-0.642708309940E-03	X4Y0	0.252277743394E-05	X6Y0	-0.169344417316E-08
X8Y0	0.557800989481E-12				
X2Y1	0.103910803976E-03	X2Y2	0.357849323060E-05	X2Y3	-0.949393451426E-07
X2Y4	-0.263665077962E-08	X2Y5	0.448024279610E-10	X2Y6	0.869676862215E-12
X4Y1	-0.818681100123E-07	X4Y2	-0.224113449347E-08	X4Y3	0.502636382929E-10
X4Y4	0.694203541988E-12	X6Y1	0.402554283956E-10	X6Y2	0.108755319609E-11
10	TILT	IN	-2.8979613	OUT	-5.3858650
K	1.000000000000E+00				
X0Y3	0.535841210347E-04	X0Y4	-0.996504125141E-05	X0Y5	0.143244090606E-06
X0Y6	-0.604299610254E-08	X0Y7	0.722219124252E-09	X0Y8	-0.413075841504E-10
X2Y0	0.159390868872E-03	X4Y0	-0.974036599480E-05	X6Y0	-0.450626242547E-08
X8Y0	-0.209304431151E-10				
X2Y1	0.418206184934E-04	X2Y2	-0.192828333768E-04	X2Y3	0.255558936870E-06
X2Y4	-0.324063577750E-07	X2Y5	0.217802590980E-08	X2Y6	-0.590627464216E-10
X4Y1	0.194313124753E-06	X4Y2	-0.251932775391E-07	X4Y3	0.229698756851E-08
X4Y4	-0.102209273990E-09	X6Y1	0.352552613064E-09	X6Y2	-0.127463275020E-09

(Table 3A continued)

	Radius of curvature	Thickness	n (540 nm)	n (450 nm)	n (630 nm)
16	TILT	IN	5.4970741	OUT	10.0708918
K	1.000000000000E+00				
X0Y3	0.614213854428E-04	X0Y4	0.294369110620E-05	X0Y5	0.260288672342E-07
X0Y6	-0.363144536866E-08	X0Y7	0.129729002187E-09	X0Y8	-0.749568185715E-11
X2Y0	-0.498779184740E-03	X4Y0	0.286914538047E-05	X6Y0	-0.230708846276E-08
X8Y0	-0.247788455504E-10				
X2Y1	0.636918236468E-04	X2Y2	0.642452002103E-05	X2Y3	-0.579769504340E-07
X2Y4	-0.125513735268E-07	X2Y5	0.743570849561E-09	X2Y6	-0.322596475353E-10
X4Y1	-0.175887764261E-07	X4Y2	-0.662208883143E-08	X4Y3	0.149128324639E-08
X4Y4	-0.104663452580E-09	X6Y1	0.493044809355E-09	X6Y2	-0.959718538659E-10
24	TILT	IN	-6.4154185	OUT	-9.5944984
K	1.000000000000E+00				
X0Y3	-0.154799685120E-04	X0Y4	-0.462492288241E-05	X0Y5	0.401758121879E-07
X0Y6	-0.179019342796E-08	X0Y7	0.884517344361E-10	X0Y8	-0.115516703562E-10
X2Y0	0.409586325200E-03	X4Y0	-0.487575661723E-05	X6Y0	-0.142834961443E-09
X8Y0	-0.230441370032E-11				
X2Y1	-0.153440934005E-04	X2Y2	-0.106723944791E-04	X2Y3	0.194829571851E-06
X2Y4	-0.351605328795E-08	X2Y5	0.431771778576E-10	X2Y6	-0.289369248321E-10
X4Y1	0.1306 59210123E-06	X4Y2	-0.564636335572E-09	X4Y3	-0.307255362585E-09
X4Y4	-0.273307738147E-10	X6Y1	-0.291791699437E-09	X6Y2	-0.130103898620E-10

Table 3B Lens data for the design (b).

	Radius of curvature	Thickness	n (540 nm)	n (450 nm)	n (630 nm)
1	-1271.3692893	217.8267780			
2	86.6405145	2.3641042	1.85996	1.89092	1.84318
3	51.1203559	5.6122709			
4	61.4834577	19.0589115	1.73460	1.74504	1.72827
5	-307.8582890	-0.0000115			
6	1341.0262896	16.7884010	1.49167	1.49637	1.48880
7	17.5535334	12.2369448			
8	-33.2995554	1.9999870	1.49167	1.49637	1.48880
9	35.0210065	0.9278805			
10	39.8979278	6.2902405	1.85722	1.87893	1.84499
11	-191.9694180	3.1322861			
12	-43.8224155	20.0000014	1.60936	1.61687	1.60482
13	-38.8724815	27.8851985			
14	945.8156609	18.9630158	1.49167	1.49637	1.48880
15	-32.1600484	5.1787813			
16	-26.0339281	2.0411681	1.73270	1.75044	1.72263
17	-105.0631300	-0.0000072			
18	88.2346790	6.6796716	1.49521	1.49998	1.49230
19	-40.0080418	3.8134937			
20	-76.3882853	1.9999983	1.53048	1.53765	1.52614
21	50.5992817	0.4424605			
22	58.9840806	7.8864811	1.49167	1.49637	1.48880
23	-46.6889043	-0.0000040			
24	28.4901823	16.6987262	1.49540	1.50018	1.49249
25	158.7100748	1.0000000			
26	INFINITY	29.0000000	1.51857	1.52485	1.51472
27	INFINITY	5.8000452			
1	TILT	IN	35.0000000	OUT	-35.0000000
K	1.000000000000E+00				
X0Y3	0.995594474623E-06	X0Y4	-0.132990492948E-07	X0Y5	-0.231816596139E-10
X0Y6	0.138297835612E-11	X0Y7	-0.215293681389E-15	X0Y8	-0.315492800003E-16

(Table 3B continued)

	Radius of curvature	Thickness	n (540 nm)	n (450 nm)	n (630 nm)
X2Y0	0.512813502760E-04	X4Y0	-0.261494615294E-08	X6Y0	0.529288128317E-13
X8Y0	0.978886055706E-18				
X2Y1	-0.142095083006E-05	X2Y2	0.533542827158E-08	X2Y3	0.225444401055E-10
X2Y4	-0.141061083607E-12	X2Y5	-0.437208518788E-15	X2Y6	0.450402541604E-17
X4Y1	0.138478688928E-09	X4Y2	-0.326603464830E-12	X4Y3	-0.882313439147E-15
X4Y4	0.171969000111E-17	X6Y1	-0.357042176093E-14	X6Y2	0.136566846152E-16
4	TILT	IN	5.4743299	OUT	9.5251405
K	1.000000000000E+00				
X0Y3	0.368475578562E-04	X0Y4	0.134191083452E-05	X0Y5	0.234570168607E-08
X0Y6	-0.342947353799E-09	X0Y7	0.140197677177E-10	X0Y8	0.174453795284E-12
X2Y0	-0.155641973840E-03	X4Y0	0.111006844309E-05	X6Y0	-0.573120990555E-10
X8Y0	-0.700510286846E-13				
X2Y1	0.557481691547E-04	X2Y2	0.178686604679E-05	X2Y3	0.832780815332E-08
X2Y4	0.384238279072E-09	X2Y5	0.192615631980E-10	X2Y6	-0.326508428988E-12
X4Y1	-0.176472379959E-07	X4Y2	0.315991481318E-09	X4Y3	0.147069553805E-10
X4Y4	-0.562900820087E-12	X6Y1	0.156505204251E-10	X6Y2	-0.388237854104E-12
11	TILT	IN	8.8040018	OUT	4.7271378
K	1.000000000000E+00				
X0Y3	-0.220079358666E-04	X0Y4	0.359358783207E-05	X0Y5	-0.748205087577E-07
X0Y6	0.326957334775E-09	X0Y7	-0.667378010318E-11	X0Y8	-0.373229816628E-11
X2Y0	-0.680153013440E-04	X4Y0	0.327710063362E-05	X6Y0	-0.655623019204E-10
X8Y0	-0.140629693345E-11				
X2Y1	-0.720574793555E-05	X2Y2	0.582801240513E-05	X2Y3	-0.799057629605E-07
X2Y4	0.908579546426E-08	X2Y5	-0.250233156809E-09	X2Y6	-0.492083281834E-10
X4Y1	-0.132759810310E-06	X4Y2	0.297133848923E-08	X4Y3	-0.317046042538E-09
X4Y4	-0.566819682147E-10	X6Y1	0.163084858971E-09	X6Y2	-0.699535688490E-11
16	TILT	IN	2.7055223	OUT	4.6913639
K	1.000000000000E+00				
X0Y3	0.843408568395E-05	X0Y4	0.972116439430E-06	X0Y5	0.745720820871E-07
X0Y6	-0.170906548181E-09	X0Y7	-0.177329936138E-10	X0Y8	0.341051119552E-11
X2Y0	-0.185957642745E-03	X4Y0	0.510516135190E-06	X6Y0	0.231039725794E-08
X8Y0	-0.123674084182E-10				
X2Y1	0.156026229631E-04	X2Y2	0.154188728555E-05	X2Y3	0.851636330240E-07
X2Y4	-0.371553197132E-08	X2Y5	0.105280972326E-09	X2Y6	0.277756732874E-10
X4Y1	0.359389756295E-07	X4Y2	0.624789202724E-08	X4Y3	0.538523111520E-09
X4Y4	-0.808703415236E-11	X6Y1	0.319751918024E-09	X6Y2	-0.434252855843E-10
25	TILT	IN	5.6221068	OUT	3.7562498
K	1.000000000000E+00				
X0Y3	-0.783350538159E-04	X0Y4	0.107389859769E-04	X0Y5	0.129655183005E-06
X0Y6	0.100444230746E-08	X0Y7	-0.525597886441E-09	X0Y8	0.145305844580E-10
X2Y0	-0.355022381745E-03	X4Y0	0.947744770084E-05	X6Y0	0.140609915829E-09
X8Y0	-0.551265632912E-11				
X2Y1	-0.535586947704E-04	X2Y2	0.200407760551E-04	X2Y3	0.287436960753E-07
X2Y4	-0.499445533732E-08	X2Y5	-0.748204525218E-09	X2Y6	0.472342541027E-10
X4Y1	-0.319823500669E-09	X4Y2	-0.571728560073E-09	X4Y3	0.253522895769E-10
X4Y4	0.877760652007E-11	X6Y1	0.295681050629E-09	X6Y2	-0.268371913684E-10

Table 3C Lens data for the design (c).

	Radius of curvature	Thickness	n (540 nm)	n (450 nm)	n (630 nm)
1	-1269.8920213	240.1165433			
2	50.0840252	8.9080866	1.85996	1.89092	1.84318
3	35.2380441	2.4732311			
4	37.0947043	16.5931564	1.73648	1.74699	1.73012

(Table 3C continued)

	Radius of curvature	Thickness	n (540 nm)	n (450 nm)	n (630 nm)
5	36.7149813	8.6478021			
6	35.9280113	2.5976070	1.49167	1.49637	1.48880
7	20.7858318	9.4244356			
8	2285.7671056	1.9999918	1.49167	1.49637	1.48880
9	38.0842174	5.7163053			
10	-79.7003555	16.7021096	1.82352	1.83772	1.81509
11	-33.6277314	3.6311479			
12	-31.0298881	20.0000053	1.49167	1.49637	1.48880
13	-72.2996396	26.7112682			
14	43.7921532	4.7924009	1.52038	1.52566	1.51717
15	-85.0350800	25.2318376			
16	-23.5266813	3.6688129	1.60964	1.62100	1.60303
17	86.2502408	-0.0000064			
18	57.8049582	6.5327970	1.49401	1.49876	1.49111
19	-26.7592615	-0.0000031			
20	101.0849523	1.9999965	1.63891	1.65141	1.63167
21	26.0668406	0.3790385			
22	28.7368482	5.8364954	1.50979	1.51485	1.50671
23	558.6536458	0.3260156			
24	27.1691412	7.8274687	1.49356	1.49830	1.49067
25	-101.3492827	1.0000000			
26	INFINITY	29.0000000	1.51857	1.52485	1.51472
27	INFINITY	5.8001567			
1	TILT	IN	35.0000000	OUT	-35.0000000
K	1.000000000000E+00				
X0Y3	0.156663799300E-05	X0Y4	-0.118890234350E-07	X0Y5	-0.771101583159E-10
X0Y6	0.111197967359E-11	X0Y7	0.966475014818E-15	X0Y8	-0.221136320326E-16
X2Y0	0.203127587644E-03	X4Y0	0.133658376319E-08	X6Y0	-0.203288563759E-12
X8Y0	0.453150117805E-17				
X2Y1	-0.122743835327E-05	X2Y2	0.496057030692E-08	X2Y3	-0.342630829479E-11
X2Y4	-0.836053949808E-13	X2Y5	0.849024027832E-15	X2Y6	-0.296551023147E-17
X4Y1	0.836373755454E-10	X4Y2	-0.108072227159E-12	X4Y3	-0.198502111248E-15
X4Y4	0.307082282034E-18	X6Y1	-0.171863596006E-14	X6Y2	0.386993744374E-17
5	TILT	IN	-23.7409583	OUT	-13.4059572
K	1.000000000000E+00				
X0Y3	-0.685261454609E-04	X0Y4	-0.294740238719E-05	X0Y5	0.731985767463E-08
X0Y6	0.940491797039E-09	X0Y7	-0.737104264968E-10	X0Y8	-0.158019971850E-11
X2Y0	0.320678212314E-02	X4Y0	-0.352098383859E-06	X6Y0	-0.274074924345E-08
X8Y0	-0.125328954712E-11				
X2Y1	-0.102960398923E-03	X2Y2	-0.108791782316E-05	X2Y3	-0.644827365580E-07
X2Y4	-0.635823927631E-08	X2Y5	-0.296738345404E-10	X2Y6	-0.971461939209E-11
X4Y1	0.156209707256E-07	X4Y2	-0.341827924853E-08	X4Y3	0.255736716760E-09
X4Y4	-0.156090011482E-10	X6Y1	-0.116621655726E-10	X6Y2	-0.140687273689E-10
10	TILT	IN	-0.3573821	OUT	-0.6517045
K	1.000000000000E+00				
X0Y3	-0.353349049564E-04	X0Y4	-0.926134011004E-05	X0Y5	0.168789646785E-06
X0Y6	-0.340410142304E-08	X0Y7	0.338123049678E-09	X0Y8	-0.374926843341E-10
X2Y0	0.417465301356E-03	X4Y0	-0.284782695666E-05	X6Y0	-0.156301035137E-07
X8Y0	0.870393401209E-11				
X2Y1	-0.979833370643E-04	X2Y2	-0.710043053102E-05	X2Y3	-0.203548420750E-06
X2Y4	-0.541160428668E-07	X2Y5	0.128754938222E-08	X2Y6	-0.552285147851E-10
X4Y1	0.126752318426E-07	X4Y2	-0.306861265581E-07	X4Y3	0.587545802267E-09
X4Y4	-0.593619012180E-10	X6Y1	0.109968704382E-09	X6Y2	-0.524096743462E-10
12	TILT	IN	-9.2666374	OUT	-13.8985063
K	1.000000000000E+00				
X0Y3	-0.861575069892E-04	X0Y4	0.491922690895E-05	X0Y5	-0.963711234923E-07

(Table 3C continued)

	Radius of curvature	Thickness	n (540 nm)	n (450 nm)	n (630 nm)
X0Y6	-0.243158270025E-08	X0Y7	0.173826351279E-09	X0Y8	0.118011235744E-10
X2Y0	-0.911884654828E-03	X4Y0	0.209463686518E-05	X6Y0	0.111487879431E-07
X8Y0	-0.126237948691E-10				
X2Y1	-0.334259497820E-04	X2Y2	0.541472857788E-05	X2Y3	0.327287937402E-07
X2Y4	0.252764894899E-07	X2Y5	0.185127111317E-09	X2Y6	-0.222987663535E-10
X4Y1	-0.274352343020E-07	X4Y2	0.255452323371E-07	X4Y3	0.103611111279E-08
X4Y4	-0.221219439871E-10	X6Y1	0.190926328083E-09	X6Y2	0.162048587926E-11
23	TILT	IN	8.5322110	OUT	5.6394864
K	1.000000000000E+00				
X0Y3	-0.622817548581E-04	X0Y4	0.703483766389E-05	X0Y5	-0.559108773014E-08
X0Y6	0.540384772196E-08	X0Y7	-0.438265263587E-10	X0Y8	0.170794172582E-10
X2Y0	-0.664734558996E-03	X4Y0	0.698920076870E-05	X6Y0	0.297309318839E-08
X8Y0	0.210579343431E-10				
X2Y1	-0.436312168709E-04	X2Y2	0.133631173155E-04	X2Y3	-0.105086584137E-06
X2Y4	0.152659067263E-07	X2Y5	0.821132599038E-10	X2Y6	0.640308844745E-10
X4Y1	-0.722722272005E-07	X4Y2	0.160462296772E-07	X4Y3	0.232108200989E-09
X4Y4	0.105344850788E-09	X6Y1	0.275764030637E-09	X6Y2	0.535411872722E-10

The sample field is number 4 (upper vertical edge on the source surface). Surface number 1 is the mirror. Surface number 25 is the surface before the prism. The overall sensitivity of the design (b) is much smaller. The large sensitivity at surfaces 21 and 22 could be reduced by cementing these surfaces. Figure 8 shows the comparison of the Monte Carlo simulation results between designs (a) and (b) under the decenter. The decenter of the surfaces is supposed to be statistically independent. The decenter of each surface is distributed uniformly between -0.02 mm and 0.02 mm. The vertical axis of the graph is the average loss of the sagittal and tangential MTF at 36 lp/mm. The effect of the sensitivity control was confirmed with the Monte Carlo simulation of the MTF.

Figure 9 shows the base functions of the surface irregularity for the control of the sensitivity to the surface irregularity [6]. These base functions are included in the base functions for the representation of the freeform surfaces [10]. These functions are axially symmetric. The axially asymmetric surface irregularity is not considered here. This is a simple model, but it is expected to be useful to get the design with the lower sensitivity to the surface irregularity. The sensitivity to the surface error corresponding to these base functions were controlled during the optimization with the traveling freeform surfaces. Figure 10 shows the comparison of the Monte Carlo simulation results between designs (b) and (c) under the surface irregularity. The RMS surface error is the order of 0.1 μm for these simulations. The sensitivity to the surface irregularity is still high, but the effect of the sensitivity control is significant. The readers may ask how the reduction of the sensitivity was achieved: with smaller deviations from the sphere, smaller gradients, smaller surface tilts, or lower angles of incidence? Unfortunately, the analysis of this reason is beyond the ability of the author. The author has been making the effort to achieve the insensitive design automatically without the considerations in detail.

Table 3A, B, and C show the lens data of designs (a), (b), and (c), respectively. The expression of the freeform surfaces was transformed to the rotationally symmetric quadric and the simple polynomials.

$$f(x,y)=\frac{c(x^2+y^2)}{1+\sqrt{1-Kc^2(x^2+y^2)}}+\sum_{i,j\geq 0}^{i+j\leq N} a_{ij}x^i y^j \qquad (5)$$

The keyword *xiyj* in the lens data indicates the coefficient a_{ij}. The keyword TILT IN indicates the tilt angle between the surface normal and the axial ray before the refraction or reflection. The keyword OUT indicates the tilt angle between the surface normal and the axial ray after the refraction or reflection.

4 Conclusion

In this paper, the method of the sensitivity control of the traveling freeform surfaces was described. The significant reduction of the tolerance sensitivity was demonstrated with a design example. The desensitization is very important for the practical use of axially asymmetric optical systems. The proposed method would be a powerful tool for this purpose.

Received October 25, 2012; accepted November 26, 2012

References

[1] G. Catalan, Appl. Opt. 33, 1907–1915 (1994).
[2] J. R. Rogers, Proc. SPIE 6342, 63420M (2006).
[3] J. P. McGuire Jr., Proc. SPIE 6342, 63420O (2006).
[4] M. Isshiki, D. C. Sinclair and S. Kaneko, Proc. SPIE 6342, 63420N (2006).
[5] A. Yabe, Appl. Opt. 49(27), 5175–5182 (2010).
[6] A. Yabe, Proc. SPIE 6342, 634225 (2006).
[7] G. W. Forbes, Opt. Express 15(8), 5218–5226 (2007).
[8] R. N. Youngworth, Proc. SPIE 7433, 74330H (2009).
[9] G. W. Forbes, Opt. Express 19(10), 9923–9941 (2011).
[10] A. Yabe, Appl. Opt. 51(15), 3054–3058 (2012).
[11] A. Yabe, Proc. SPIE 8167, 816703 (2011).
[12] A. Yabe, Proc. SPIE 3482, 122–125 (1998).
[13] A. Yabe, Appl. Opt. 50(19), 3369–3374 (2011).
[14] A. Yabe, Proc. SPIE 4832, 206–217 (2002).

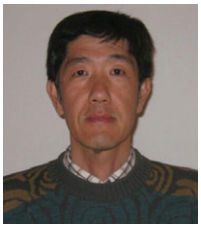

Akira Yabe received his BSc in Physics from Tokyo University in 1978. He worked for Fuji Photo Optical (1978–2003). He is a lens design consultant (2004–). His experience of lens design ranges from the cinematography zoom lens to the microlithography lens. He works with his own lens design code. He has unique methods of the optical design, such as prototyping of zoom lenses, global optimization, optimal selection of aspheric surfaces, accurate glass model and cost control, sensitivity control, and determination of tolerances.